Pflugers Arch - Eur J Physiol (2008) 455:1041–1054
DOI 10.1007/s00424-007-0364-6

CELL AND MOLECULAR PHYSIOLOGY

# Missorting of the Aquaporin-2 mutant E258K to multivesicular bodies/lysosomes in dominant NDI is associated with its monoubiquitination and increased phosphorylation by PKC but is due to the loss of E258

**Erik-Jan Kamsteeg · Paul J. M. Savelkoul · Giel Hendriks · Irene B. M. Konings · Nicole M. I. Nivillac · Anne Karine Lagendijk · Peter van der Sluijs · Peter M. T. Deen**

Received: 4 July 2007 / Revised: 28 August 2007 / Accepted: 2 October 2007 / Published online: 27 October 2007


**Abstract** To stimulate renal water reabsorption, vasopressin induces phosphorylation of Aquaporin-2 (AQP2) water channels at S256 and their redistribution from vesicles to the apical membrane, whereas vasopressin removal results in AQP2 ubiquitination at K270 and its internalization to multivesicular bodies (MVB). AQP2-E258K causes dominant nephrogenic diabetes insipidus (NDI), but its subcellular location is unclear, and the molecular reason for its involvement in dominant NDI is unknown. To unravel these, AQP2-E258K was studied in transfected polarized Madin–Darby canine kidney (MDCK) cells. In MDCK cells, AQP2-E258K mainly localized to MVB/lysosomes (Lys). Upon coexpression, wild-type (wt) AQP2 and AQP2-E258K formed multimers, which also localized to MVB/Lys, independent of forskolin stimulation. Orthophosphate labeling revealed that forskolin increased phosphorylation of wt-AQP2 and AQP2-E258K but not AQP2-S256A, indicating that the E258K mutation does not interfere with the AQP2 phosphorylation at S256. In contrast to wt-AQP2 but consistent with the introduced protein kinase C (PKC) consensus site, AQP2-E258K was phosphorylated by phorbol esters. Besides the 29-kDa band, however, an additional band of about 35 kDa was observed for AQP2-E258K only, which represented AQP2-E258K uniquely monoubiquitinated at K228 only. Analysis of several mutants interfering with AQP2-E258K phosphorylation, and/or ubiquitination, however, revealed that the MVB/lysosomal sorting of AQP2-E258K occurred independent of its monoubiquitination or phosphorylation by PKC. Instead, our data reveal that the loss of the E258 in AQP2-E258K is fundamental to its missorting to MVB/Lys and indicate that this amino acid has an important role in the proper structure formation of the C-terminal tail of AQP2.

**Keywords** Water channel · AQP2 · Phosphorylation · Membrane trafficking · Ubiquitination

E.-J. Kamsteeg · P. J. M. Savelkoul · I. B. M. Konings · N. M. I. Nivillac · A. K. Lagendijk · P. M. T. Deen (✉)
Department of Physiology, Radboud University Nijmegen Medical Center,
Research Tower, 7th floor; UMC St Radboud,
P.O. Box 9101, 6500 HB Nijmegen, The Netherlands
e-mail: p.deen@ncmls.ru.nl

G. Hendriks · P. van der Sluijs
Department of Cell Biology, UMC Utrecht,
Utrecht, The Netherlands

## Introduction

Regulating water homeostasis in the body is one of the major features of the mammalian kidney. From the vast amount of prourine adult humans produce each day (180 l), most of the water content is constitutively reabsorbed in the renal proximal tubules and descending limbs of Henle. Uptake of the remaining water, which still is 10–20 l per day, is under tight control of the antidiuretic hormone arginine vasopressin (AVP). Upon hypernatremia or hypovolemia, AVP is released from the pituitary and binds to its vasopressin type-2 receptor (V2R) in the basolateral membranes of principal and inner medullary collecting duct cells. This binding initiates a cyclic adenosine monophosphate (cAMP) signaling cas-

cade, which leads to the phosphorylation of the Aquaporin-2 (AQP2) water channel at Ser256 and presumably other proteins. Subsequently, intracellular vesicles containing AQP2 fuse with the apical membrane enabling water to enter the cell via the apical membrane and leave the cell via AQP3 and AQP4 water channels located at the basolateral membrane [8, 42].

In acquired and congenital nephrogenic diabetes insipidus (NDI), the AVP-induced renal water reabsorption is impaired, and urine is not efficiently concentrated, although blood AVP levels are often increased [34]. In congenital NDI, mutations in the *V2R* gene (*AVPR2*; NM_000054.2) cause the X-linked form, while mutations in the *AQP2* gene (NM_000486.3) cause the autosomal recessive and dominant forms of NDI [1–3, 7, 27, 29, 35, 39, 47, 48]. Mutations in the *AQP2* gene in recessive NDI lead to AQP2 proteins that are retained in the endoplasmic reticulum (ER), presumably because of misfolding [4, 25]. Their inability to form oligomers, which is a normal characteristic of wild-type (wt) AQP2, also precludes interaction with wt-AQP2 [18, 21]. The unaffected sorting of wt-AQP2 in the presence of these mutants provides an explanation for the recessive nature of inheritance.

The first *AQP2* mutation identified in dominant NDI was c.772G>A (p.Glu258Lys). Expression studies in *Xenopus laevis* oocytes revealed that this mutant, referred to as AQP2-E258K, is not retained in the ER but was missorted to the Golgi complex region, whereas wt-AQP2 in these cells is always in the plasma membrane [29]. Furthermore, AQP2-E258K was able to heteroligomerize with wt-AQP2 and keep this wt/mutant oligomer from the plasma membrane, explaining the dominant inheritance of NDI [21]. Subsequent analysis of other AQP2 mutants revealed that heteroligomerization and missorting of the wt-AQP2/mutant complexes is the common cellular mechanism in dominant NDI [17, 23, 26]. The subcellular organelle in which AQP2-E258K alone or when complexed with wt-AQP2 resides remained unclear. Moreover, the molecular mechanism by which AQP2-E258K causes dominant NDI is unknown. Because oocytes are not epithelial cells, some AQP2 mutants in dominant NDI are sorted to other subcellular destinations in these cells than in epithelial cells, and wt-AQP2 is constitutively phosphorylated in oocytes, these cell may not represent the best model to analyze AQP2-E258K. In contrast, Madin–Darby Canine Kidney (MDCK) cells are derived from renal collecting ducts [16] and display similar regulation of exogenous AQP2 as observed in vivo (i.e., AVP causes AQP2 translocation from intracellular vesicles to the apical plasma membrane) [5]. Therefore, we here characterized the subcellular localization of AQP2-E258K, its role in dominant NDI, and the molecular reason for its involvement in dominant NDI in detail in the MDCK cells.

## Materials and methods

### Expression constructs

For expression in MDCK cells, the AQP2-E258K cDNA fragment was digested from pT7Ts-AQP2-E258K [29] with *Spe*I and *Bgl*II and cloned into the *Bgl*II and *Xba*I sites of pCB6. To generate a eukaryotic expression construct encoding FLAG-tagged wt-AQP2 (F-AQP2), pBSKSII+-F-AQP2 [21] was digested with *Not*I, blunted and digested with *Hin*dIII, and the obtained F-AQP2 cDNA fragment was ligated into the *Hin*dIII and blunted *Kpn*I site of pCB7ΔBHI, which also contains a hygromycin resistance cassette. The construct encoding F-AQP2-E258K was made from the latter one by replacement of the internal *Bam*HI–*Kpn*I AQP2 cDNA fragment with that of pT7Ts-AQP2-E258K. To create cDNAs that encode the ubiquitination-defective or phosphorylation state-specific mutants, desired mutations were introduced by the QuickChange in vitro mutagenesis system, followed by sequencing and subcloning of the mutated cDNA fragments. Electronic files of the constructs are available upon request.

### Cell culture and transfection

MDCK type I cells expressing wt-AQP2, AQP2-S256A, GFP-AQP2, or AQP2-Ub have been described [5, 20, 26]. MDCK cells were grown and stably transfected as described [6]. For hygromycin selection, a concentration of 75 μg/ml was used for up to 10 days. To select representative stably transfected cell lines, the obtained clones were analyzed for expression of the heterologous protein by immunoblotting and proper morphology of the cells. Subsequently, of at least four independent clones, the intracellular localization of the expressed protein was determined by immunocytochemistry and confocal laser scanning microscopy (CLSM). For this, cells were pre-incubated overnight with $5\times10^{-5}$ M of the prostaglandin synthesis inhibitor indomethacin, to reduce basal intracellular cAMP levels, and incubated the next day with or without $5\times10^{-5}$ M of the adenylate cyclase-activating drug forskolin (in the presence of indomethacin) to induce AQP2 translocation to the apical membrane [5]. When the subcellular localization pattern was consistent for at least three out of four clones, one or two of these clones were selected for further studies.

For transient transfection, cells were seeded at a density of $1.5\times10^{5}/cm^{2}$. The next day, these cells were transfected using Lipofectamine 2000 reagent (Invitrogen, Carlsbad, CA). For this, 1.5 μg of DNA and 4.5 μg Lipofectamine2000 per $cm^{2}$ of cell culture dish was separately diluted with Opti-MEM I medium (Biowithaker, Europe) and left for 5 min. Subsequently, the two solutions were

mixed, left at room temperature for 15 min, dropwise added to the culture dish containing the cells, and left for 3 h at 37°C. Subsequently, the mixture was removed, and cells were grown further in Dulbecco's modified Eagle's medium (DMEM) with 5% fetal calf serum for 3 days after which they were immunocytochemically analyzed. Stable clones from these transfections were obtained by picking single clones after growth on selection drug for 10 days. A minimum of three cell lines per mutant were analyzed for consistency of results.

COS-7 cells were grown in alpha-modified Eagle's medium (MEM), supplemented with 10% fetal bovine serum and 2mM L-glutamine, and were transfected with Lipofectamin-2000 (Invitrogen).

### Side-specific biotinylation, orthophosphate, and pulse-chase labeling, and immunoprecipitation

Side-specific biotinylation [6] and orthophosphate labeling [45] of AQP2-expressing cells were performed as described. Where indicated, forskolin ($10^{-5}$ M) or Phorbol 12-myristate 13-acetate (PMA, $10^{-7}$ M) were added to the in culture medium. Before the experiments, the cells were incubated overnight with indomethacin ($5\times10^{-5}$ M). For pulse-chase labeling, cells were grown in 6-cm tissue culture dishes, washed with phosphate-buffered saline (PBS) and incubated for 30 min with methionine- and cysteine-free MEM (Sigma, St. Louis, MO). The cells were labeled for 30 min at 37°C with 0.2 mCi/ml 35S methionine/cysteine (Redivue Promix, Amersham) and chased for different periods of time in DMEM, 10% fetal calf serum, 1 mM methionine, and 1 mM cysteine. Cells were lysed in 1 ml 1% Triton X-100, 50 mM Tris pH 7.4, 1 mM ethylene diamine tetraacetic acid, and a protease inhibitor mix (Complete mini, Roche) on ice. Detergent lysates were centrifuged at 14,000 rpm for 5 min to remove insoluble debris. Next, lysates were precleared by incubation with bovine serum albumin (BSA)-coated protein A beads for 1 h at 4°C. The supernatants were then transferred to a fresh tube and incubated with anti AQP2 antibody-coated beads for 2 h at 4°C. Beads were washed three times at room temperature for 5 min with 0.05% Triton X-100, 0.1% sodium dodecyl sulfate (SDS), 0.3 M NaCl, 10 mM Tris–HCl pH 8.6, and then resuspended in 25 μl Laemmli sample buffer (2% SDS, 50 mM Tris, pH 6.8, 12% glycerol, 0.01% Coomassie Brilliant Blue, 100 mM dithiothreitol).

For immunoprecipitations in orthophosphate-labeling experiments, 10 μl protein A agarose beads (Kem-En-Tec A/S, Copenhagen, Denmark) per sample was washed twice in lysis buffer, 1% BSA. Per sample, 4 μl of rabbit 7 anti-AQP2 antibodies was added to protein-A beads in 400 μl lysis buffer and rotated overnight at 4°C. These antibodies were raised against the 15 COOH-terminal amino acids of rat AQP2 [4]. Then, the protein A-antibody beads were washed twice in ice-cold lysis buffer and incubated with cell supernatant for 16 h after washing four times with lysis buffer containing phosphatase inhibitors, proteins were liberated from the beads using 30 μl of Laemmli sample buffer. Proteins were incubated for 30 min at 37°C and resolved by SDS-polyacrylamide gel electrophoresis (PAGE) on 12.5% gels. Quantification of immunoprecipitated AQP2 was done by phosphoimaging (pulse-chase labeling) or by comparison of densitometrically scanned immunoblot signals with a two-fold dilution series of wt-AQP2/AQP2-E258K. Analysis of variance (ANOVA) analyses was used to calculate the $p$ value of the differences between groups.

### SDS-PAGE and immunoblotting

Protein samples were denatured, separated by SDS-PAGE, and immunoblotted as described [4]. Primary antibodies used were: affinity-purified rabbit AQP2 antibodies [4] diluted 1:3,000 in Tris-buffered saline–Tween-20 (TBS-T) and ubiquitin monoclonal antibodies (SPA 203, Stressgen Biotechnologies, Canada; or Ubu-1, Zymed, San Francisco, CA) diluted 1:2,000 in TBS-T with 5% nonfat dried milk. Subsequently, goat anti-rabbit antibodies (1:5,000 in TBS-T, Sigma) or sheep anti-mouse antibodies (1:2,000 in TBS-T, Sigma), both coupled to horse radish peroxidase, were used. Proteins were visualized using enhanced chemiluminescence (Pierce). SDS-polyacrylamide gels loaded with $^{32}$P-labeled samples were dried before exposure to film.

### Immunocytochemistry

Growth of cells, their treatment with indomethacin and forskolin, and immunocytochemistry were performed as reported [6] A 1:100 dilution of affinity-purified rabbit anti-AQP2 antibodies, guinea pig anti-AQP2 antibodies, or monoclonal antibodies against FLAG (M2, Sigma) were used alone or in combination with one of the following organelle marker antibodies: 1:100 dilution of rabbit anti GOS28 antibodies [41] and 1:100 dilution of monoclonal antibodies against Golgi 58K protein (Sigma) or 1:200 dilution of monoclonal antibodies (clone AC17) against the late endosomal/lysosomal marker Lamp2 [31] (kindly provided by Dr. Le Bivic, Marseille, France). All antibodies were diluted in goat serum dilution buffer (GSDB; PBS containing 16% goat serum, 0.3% Triton-X100 [except for the Lamp2 antibodies, which were in 0.3% saponin], 0.1% BSA, and 300 mM NaCl). For labeling lysosomes (Lys), the cells were loaded with 75 nM LysoTracker Red DND-99 (Molecular Probes Eugene, OR) for 90 min before fixation with paraformaldehyde, according to the manufacturer's protocol. Subsequently, the filters were incubated

with a 1:100 dilution of secondary antibodies coupled to a fluorescent dye (Alexa Fluor ™ 594 or 488 goat anti-rabbit, goat anti-guinea pig or goat anti-mouse, Molecular Probes) or goat anti-mouse Cy5 antibodies (Sigma) in GSDB for 45 min. Next, filters were washed and mounted on glass slides with Vectashield (Vector Labs, Burlingame, CA). Images were obtained with a Bio-Rad confocal laser scanning imaging system using a ×60 oil-immersion objective. As a control, nontransfected MDCK cells revealed no labeling (data not shown).

### Densitometrical analysis

Each signal was scanned with a GS-690 Imaging Densitometer (Biorad, California, USA) and quantified with the "molecular analyst" analysis program. Only signals in the linear exposure range of the films were used. The densities of the twofold dilution series of wt-AQP2 were used as a (linear) standard for semiquantification of the amounts of expressed AQP2 (in arbitrary units).

## Results

### In MDCK cells, AQP2-E258K is retained in multivesicular bodies/lysosomes

To establish in which organelle(s) AQP2-E258K locates, several stably expressing MDCK cell lines were selected, and a representative clone was used in further experiments. To determine the cAMP responsiveness of AQP2-E258K, MDCK-AQP2-E258K cells were pretreated with indomethacin and subsequently stimulated with forskolin or not and subjected to immunocytochemistry with AQP2 antibodies. Subsequent CLSM analysis revealed that with or without forskolin stimulation, AQP2-E258K was localized in vesicular structures (Fig. 1a, upper panel). As shown before [5], wt-AQP2 is localized in intracellular vesicles without stimulation but is translocated to the apical membrane after forskolin stimulation (Fig. 1a, lower panel). Cell surface biotinylation assays confirmed the absence of apical surface expression of AQP2-E258K before and after forskolin stimulation and the increase in apical surface expression of wt-AQP2 after forskolin stimulation (Fig. 1b). The absence of apical AQP2-E258K expression was not due to a low expression level because this mutant was expressed at higher levels than wt-AQP2 (Fig. 1b).

To analyze the subcellular localization of AQP2-E258K further, MDCK-AQP2-E258K and unstimulated MDCK-AQP2 cells were subjected to colocalization studies using several antibodies against organelle marker proteins in combination with AQP2 antibodies. CLSM analysis revealed that both AQP2-E258K and wt-AQP2 did not colocalized with

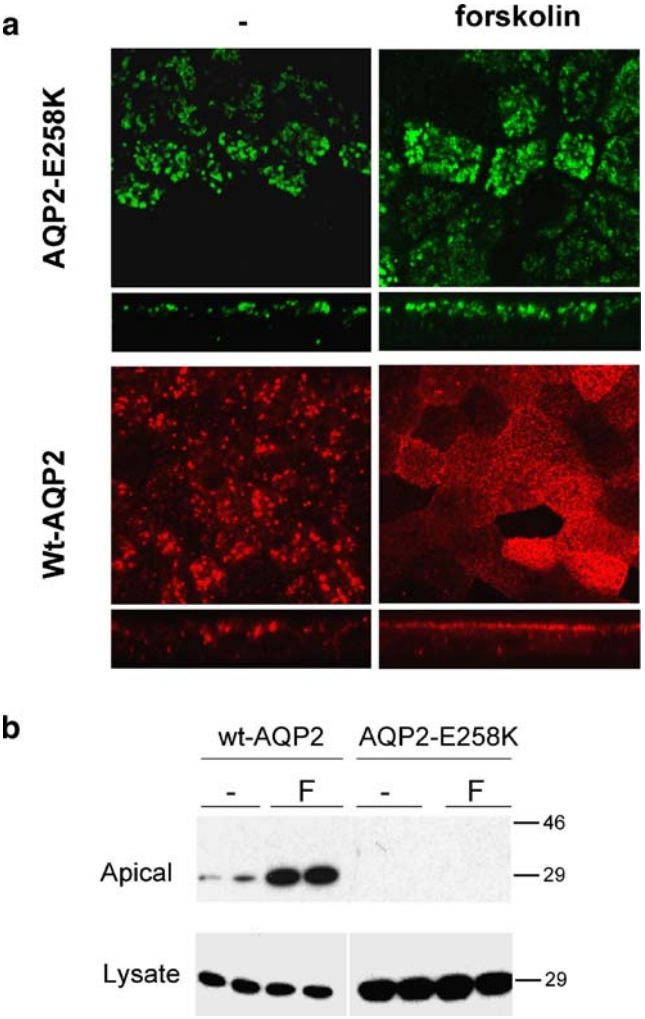


**Fig. 1** AQP2-E258K retains in intracellular vesicles in MDCK cells after stimulation of the PKA pathway. **a** MDCK cells expressing wt-AQP2 or AQP2-E258K were grown to confluence on semipermeable filters, pretreated with indomethacin and left untreated (*minus sign*) or treated for 45 min with forskolin (*forskolin*). After fixation and permeabilization, the filters were incubated with rabbit anti-AQP2 antibodies and then with Alexa 594 (wt-AQP2 cells) or Alexa 488 (AQP2-E258K cells) conjugated anti-rabbit antibodies. Confocal images were made in the XY and XZ planes. **b** MDCK cells expressing wt-AQP2 or AQP2-E258K (indicated) were grown as under **a**, left untreated (*minus sign*) or were treated with forskolin (*F*) and subjected to apical cell surface biotinylation assays. Biotinylated proteins were precipitated with streptavidin–agarose beads and immunoblotted for AQP2 (*apical*). A sample of the lysed cells was immunoblotted in parallel to visualize the amount of AQP2 protein expressed (*lysate*). The mass of the observed proteins is indicated in kDa on the *right*

marker proteins for the *cis*- (GOS28; Fig. 2a), medial- (Mannosidase II) or *trans*- (Giantin, 58K) Golgi complex before or after forskolin stimulation (not shown). However, a substantial overlap of AQP2-E258K but not wt-AQP2 expression was observed with the multivesicular bodies (MVB)/Lys marker Lamp2 (Fig. 2b). This localization of AQP2-E258K did not change with forskolin treatment (not shown).

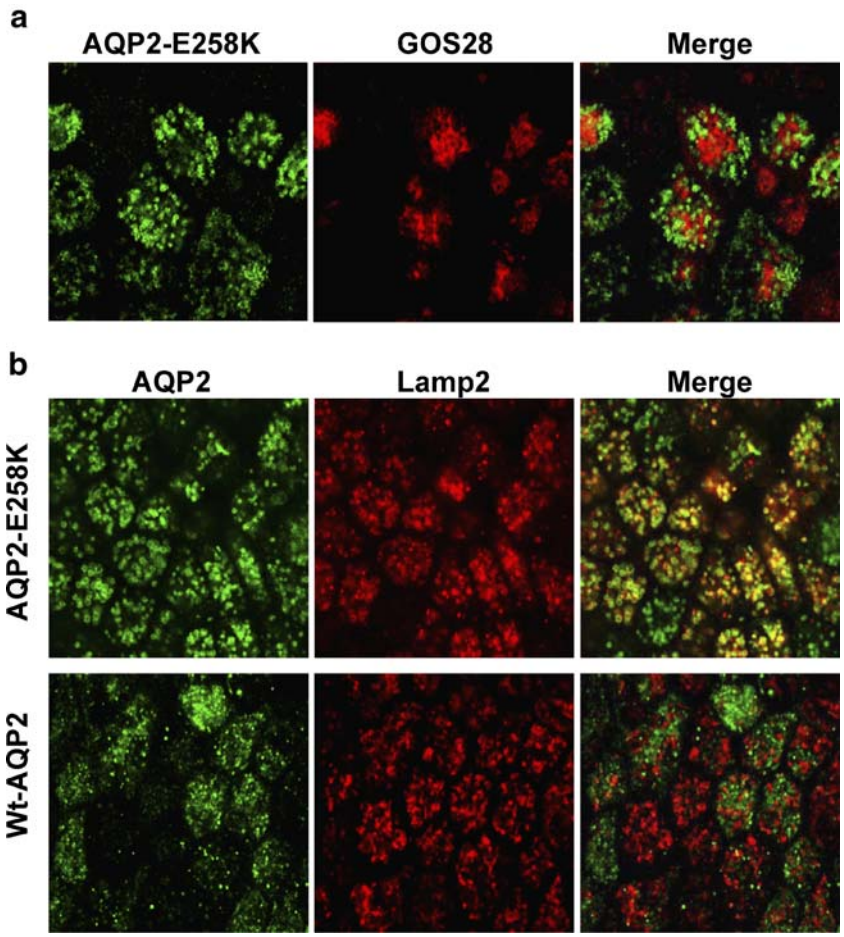


**Fig. 2** AQP2-E258K is missorted to and retains wild-type AQP2 in multivesicular bodies/lysosomes. **a**–**d** MDCK cells stably expressing different AQP2 proteins were grown and treated as described in the legend of Fig. 1. **a** MDCK-AQP2-E258K (indicated on the *top*) cells were incubated with guinea-pig AQP2 and rabbit GOS28 antibodies, followed by Alexa 488 conjugated anti-guinea pig and Alexa 594 conjugated anti-rabbit IgGs. Shown are the single (*AQP2*, *GOS28*) and merged (*Merge*) images. **b** MDCK cells stably expressing wt-AQP2 or AQP2-E258K (indicated on the *left*) were incubated with rabbit AQP2 antibodies and monoclonal antibodies recognizing the MVB/Lys marker protein Lamp2, followed by Alexa 488 conjugated anti-rabbit and Alexa 594 conjugated anti-mouse IgGs. Shown are the single (*AQP2*, *Lamp2*) and merged (*Merge*) images. **c** MDCK cells stably expressing GFP-tagged AQP2 (*G-AQP2*) were transiently transfected with an expression construct encoding FLAG-tagged AQP2-E258K (*F-AQP2-E258K*). Cells were subjected to immunocytochemistry with mouse FLAG antibodies, followed by Alexa 594-labelled secondary antibodies. **d** The same cells as in **c** were incubated with LysoTracker Red (*LysoTracker*) for 90 min before the cells were fixed. Then, the filters were subjected to immunocytochemistry with monoclonal antibodies against FLAG, followed by Cy5 conjugated anti-mouse antibodies. Shown are the single and merged (*merge*) images

## Upon coexpression, AQP2-E258K retains wt-AQP2 in MVB/Lys

In *Xenopus* oocytes, heteroligomerization of expressed wt-AQP2 and AQP2-E258K resulted in a reduced plasma membrane expression of wt-AQP2 [29], but the subcellular localization of the complex was not studied. To visualize double- and wt-AQP2-only-transfected cells in one preparation, MDCK cells stably expressing green fluorescent protein (GFP)-tagged wt-AQP2 (G-AQP2) were transfected with F-AQP2-E258K and subjected to immunocytochemistry using FLAG antibodies. CLSM analysis revealed that in cells expressing both proteins, G-AQP2 and F-AQP2-E258K mainly colocalized in an intracellular compartment, independent of forskolin stimulation (Fig. 2c). In contrast and as shown before [25], in cells only expressing G-AQP2, it localizes in the apical membrane, again independent of forskolin stimulation (Fig. 2c).

Treatment of MDCK cells with LysoTracker Red, a fluorescent compound that accumulates in acidic compartments like Lys [43], followed by immunocytochemistry using FLAG antibodies revealed that heteroligomers of G-AQP2 (green signal) and F-AQP2-E258K (blue signal) localize to MVB/Lys (Fig. 2d; with equal intensities of green, blue, and red; white signals are obtained in the merge). Again, this colocalization of G-AQP2 and F-AQP2-E258K in MVB/Lys was not changed by forskolin stimulation (not shown). Taken together, these data indicate that upon coexpression in MDCK cells, F-AQP2-E258K heteroligomerizes with wt-AQP2 and missorts the complex primarily to MVB/Lys.

## AQP2-E258K displays a decreased half-life compared to wt-AQP2

Because mature proteins targeted for degradation are sorted to MVB/Lys, we determined whether AQP2-E258K is less stable than wt-AQP2. To investigate this, MDCK cells expressing AQP2-E258K or wt-AQP2 were subjected to radio-labeled pulse-chase experiments. After a pulse of 30 min and a subsequent chase of several time periods, the cells were lysed, and AQP2 proteins were immunoprecipitated and subjected to SDS-PAGE. Autoradiographs of the gel revealed the typical bands for unglycosylated (29 kDa), high-mannose glycosylated (32 kDa), and complex-glycosylated (40–45 kDa) bands of both wt-AQP2 and AQP2-

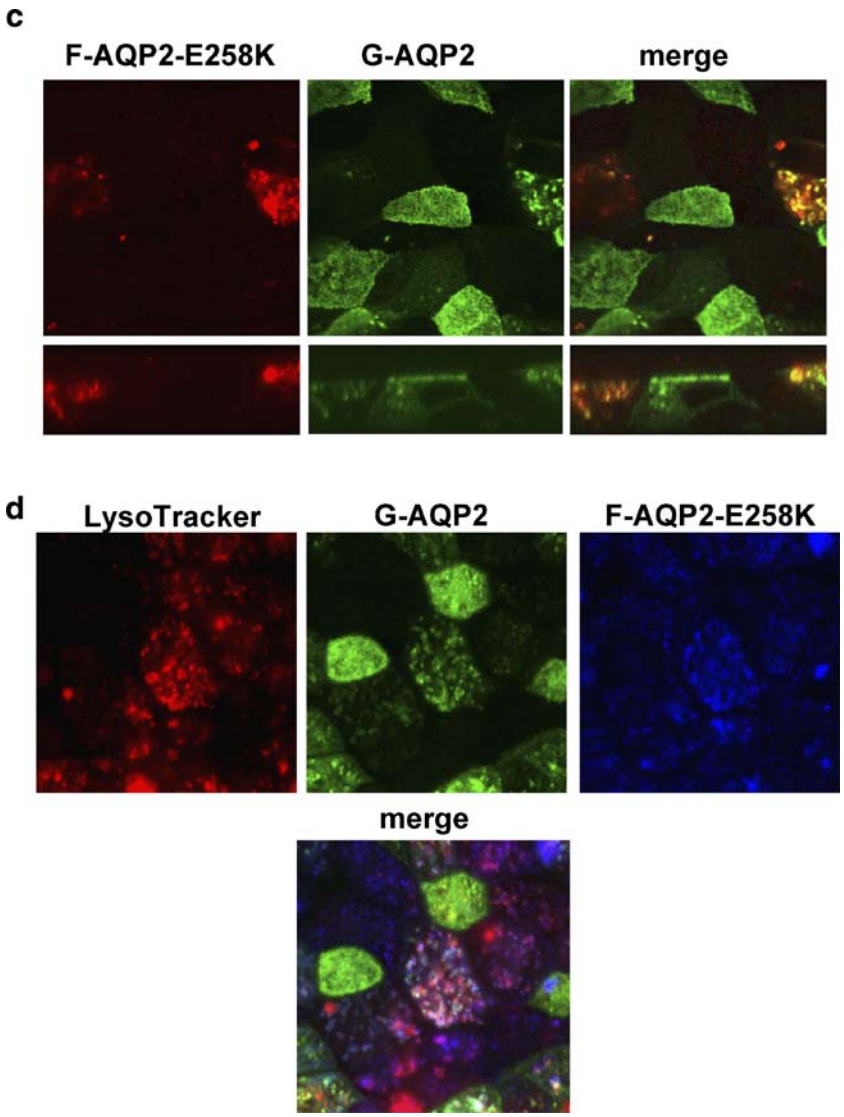


**Fig. 2** (continued)

E258K (Fig. 3a). It is interesting to note that a weak additional band of ~35 kDa was observed after 1, 3, and 6 h of chase for AQP2-E258K only (Fig. 3a, arrow). Phosphoimager quantification analysis of the 29 kDa signals (Fig. 3b) revealed that the half-life of AQP2-E258K is about 7 h, while this is about 12 h for wt-AQP2, as reported [13]. Inhibition of lysosomal degradation with chloroquin abolished the difference in degradation between wt-AQP2 and AQP2-E258K, as reported [14]. This indicated that AQP2-E258K is less stable than wt-AQP2 because of lysosomal degradation.

## Putative mechanisms underlying the missorting of AQP2-E258K

Next, we wished to identify a possible cause of the missorting of AQP2-E258K to MVB/Lys. Three putative causes for the missorting come to mind. (1) Because the E258K mutation is close to S256, which phosphorylation by (presumably) protein kinase A (PKA) is essential for translocation of AQP2 to the plasma membrane [9, 19, 22, 45], the E258K mutation could interfere with S256 phosphorylation. In addition, the E258K mutation introduces a putative protein kinase C (PKC) phosphorylation site (SXK/R). As wt-AQP2 is not phosphorylated by PKC, as analyzed after PMA treatment [45], a change in phosphorylation of AQP2-E258K by PKA and/or PKC could be fundamental to its missorting. (2) Ubiquitination is a post-translational modification of lysine residues and has a role in endocytosis and subsequent lysosomal degradation. wt-AQP2 is short-chain ubiquitinated, which induces its endocytosis and subsequent sorting to MVB/Lys [20]. Therefore, AQP2-E258K missorting could be caused by additional ubiquitination of the introduced lysine at position

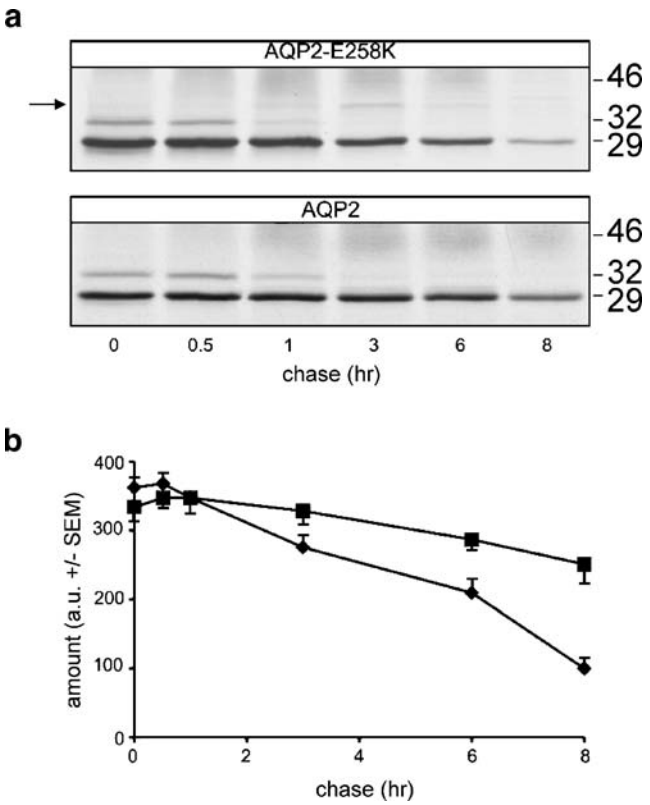


**Fig. 3** *AQP2-E258K is less stable than wt-AQP2*. **a** MDCK cells expressing wt-AQP2 or AQP2-E258K were subjected to radio-labeled pulse-chase experiments. After a pulse of 30 min and a chase for the indicated time points, the cells were lysed. AQP2 proteins were precipitated and subjected to SDS-PAGE. The *arrow* points at the ~35-kDa form of AQP2-E258K. The mass of the observed proteins are indicated in kDa on the *right*. **b** Quantification of the non-glycosylated AQP2 signals (29 kDa) from three experiment (of which **a** is representative) was done with a phosphoimager and plotted in arbitrary units (*amount (a.u.+/-SEM)*). ANOVA analysis indicated that the difference between wt-AQP2 and AQP2-E258K was significant ($p<0.01$). The *diamonds* indicate AQP2-E258K, whereas the *squares* indicate wt-AQP2

258, resulting in increased endocytosis and lysosomal targeting. (3) The glutamic acid at position 258 may be essential for proper sorting.

## Increased phosphorylation by the protein kinase C pathway and monoubiquitination of AQP2-E258K

To determine whether AQP2-E258K lacks phosphorylation by PKA or is phosphorylated by PKC, MDCK cells expressing AQP2-E258K, wt-AQP2, or AQP2-S256A (which cannot be phosphorylated at position 256) were subjected to orthophosphate labeling, left untreated, or treated with forskolin, PMA, or both forskolin and PMA. After lysis and AQP2 immunoprecipitation, half of each sample was subjected to SDS-PAGE and the gel exposed to film (Fig. 4a, top), while the other half was immunoblotted for AQP2 (Fig. 4a, middle). Forskolin treatment resulted in an increased level of phosphorylation of both wt-AQP2 and AQP2-E258K (Fig. 4a), indicating that both proteins are phosphorylated by PKA. It is interesting to note that PMA indeed increases the phosphorylation of AQP2-E258K (Fig. 4a). Moreover, PMA and forskolin have an additive effect on the phosphorylation of AQP2-E258K. The increased signal of phosphorylated AQP2 was not due to increased expression levels because the Western blot revealed similar total AQP2 levels for all conditions. The control, AQP2-S256A, was well expressed but was not

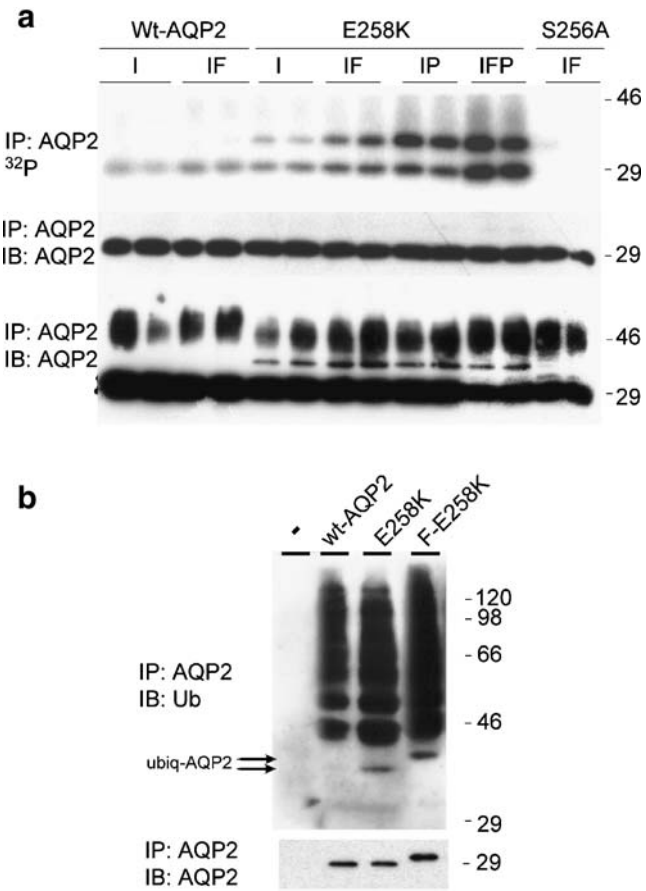


**Fig. 4** AQP2-E258K phosphorylation by PKA and PKC, and its mono-ubiquitination. **a** Cells expressing wt-AQP2, AQP2-E258K (*E258K*), or AQP2-S256A (*S256A*) were grown, treated with only indomethacin (*I*) or together with forskolin (*IF*), PMA (*IP*), or both (*IFP*) for 3 h, after $^{32}$[P]-orthophosphate labeling. Then, the cells were lysed and the AQP2 proteins were immunoprecipitated (*IP: AQP2*). The immunoprecipitates were split in two portions of which one was separated on SDS-PAGE and autoradiographed ($^{32}$P), while the other was immunoblotted for AQP2 (*IB: AQP2*, *middle panel*). An identical experiment was performed in parallel, of which the immunoprecipitates were not split into two portions but immunoblotted entirely, followed by a long exposure (*bottom panel*) **b** Nontransfected MDCK cells (*minus sign*) or those expressing wt-AQP2, AQP2-E258K, or F-AQP2-E258K were grown to confluence, lysed, and subjected to AQP2 immunoprecipitation (*IP: AQP2*). Subsequently, 90% of each sample was immunoblotted for ubiquitin (*IB: Ub*), while 10% was immunoblotted for AQP2 (*IB: AQP2*). The mass of marker proteins is given in kDa on the *right*

labeled after forskolin treatment, indicating that orthophosphate labeling of wt-AQP2 and AQP2-E258K occurred at S256.

Interestingly and consistent with the pulse-chase experiments (Fig. 3), AQP2-E258K showed an additional band of about 35 kDa in the orthophosphate-labeling experiments (Fig. 4a, top) and with AQP2 immunoblotting after amplification of the immunoblot signal and a long exposure time (Fig. 4a, lower panel). This indicates that a pool of AQP2-E258K is not only phosphorylated, but also modified otherwise. Because ubiquitin has a size of about 7–9 kDa, the observed 35-kDa protein could represent monoubiquitinated AQP2-E258K. To test this, cells expressing wt-AQP2, AQP2-E258K, or F-AQP2-E258K were grown to confluence, lysed, and subjected to AQP2 immunoprecipitation. The sample was split into two fractions of which one was immunoblotted for ubiquitin, while the other was immunoblotted for AQP2. Ubiquitin detection indeed revealed a band of 35 kDa in the lane of AQP2-E258K (Fig. 4b, arrows), which was not present in the lane of wt-AQP2. Importantly, an ubiquitinated band of about 37 kDa was detected in the lane of F-AQP2-E258K cells, which is consistent with a 2-kDa increase in size of monoubiquitinated AQP2-E258K because of the FLAG tag. The absence of monoubiquitinated wt-AQP2 was not due to differences in total immunoprecipitated AQP2 (Fig. 4b, bottom). Besides these bands, many higher ubiquitinated bands of similar sizes (Fig. 4b, top) were detected in the lanes of all three AQP2 proteins. These bands were AQP2 specific as no ubiquitinated proteins were detected in AQP2 immunoprecipitates from untransfected cells (Fig. 4b, left lane).

Altogether, these data revealed that the E258K mutation does not interfere with S256 phosphorylation by PKA but introduces S256 phosphorylation by PKC and additional monoubiquitination.

## Prevention of AQP2-E258K-specific ubiquitination, which occurs at K228, still targets AQP2-E258K to multivesicular bodies/lysosomes

Monoubiquitination at K270 targets wt-AQP2 to MVB [20]. Therefore, to determine whether the increased monoubiquitination of AQP2-E258K causes its missorting, we changed, besides K258 itself, each luminal lysine (K228, K238, and K270) in AQP2-E258K into an arginine. Besides, we also replaced all four lysines by an arginine (AQP2-4K>R). After transient expression of these constructs, wt-AQP2 and AQP2-E258K in COS-7 cells, the AQP2 proteins were immunoprecipitated and immunoblotted for AQP2. It is surprising to note that a lack of monoubiquitination was only observed for AQP2-K228R and AQP2-4K>R, indicating that AQP2-E258K is monoubiquitinated only at K228 (Fig. 5a). This absence was not due to reduced expression levels because similar 29-kDa expression levels were found (Fig. 5a). Subsequently, MDCK cell lines stably expressing AQP2-K228R-E258K or AQP2-4K>R were generated, grown to confluence, and lysed, in parallel with cell lines stably expressing wt-AQP2, AQP2-E258K, and AQP2-K270R-Ub (a constitutively monoubiquitinated form of AQP2 [20]). As shown before, immunoblotting for ubiquitin of AQP2-specific immunoprecipitates of the latter cells revealed the mono-ubiquitinated form of AQP2-K270R-Ub of 37 kDa, the mono-, di-, and triubiquitinated forms of wt-AQP2 (of about 37, 43, and 50 kDa, respectively), and a higher molecular weight smear of ubiquitinated AQP2, all specific for ubiquitination at K270 [20] (Fig. 5b). AQP2-E258K showed the same di- and triubiquitinated and higher-molecular-weight forms as wt-AQP2, albeit to a lower extent, but also revealed the ~35-kDa form specific for this mutant. The absence of only the 35-kDa form in AQP2-K228R-E258K compared to AQP2-E258K confirms that this band is due to one ubiquitin moiety coupled to the new ubiquitination target site K228. The absence of all ubiquitinated bands with AQP2-4K>R reveals that with these four changes, ubiquitination of AQP2 is completely prevented. Reprobing the blot with AQP2 antibodies revealed that this absence was not due to a reduced expression level of AQP2-4K>R (Fig. 5b, bottom panel). The reason for the difference in migration patterns of monoubiquitinated K270-conjugated wt-AQP2 (~37 kDa) and that of monoubiquitinated K228-conjugated AQP2-E258K (~35 kDa) is not clear but may be due to the fact that K270 is the penultimate amino acid of AQP2, resulting in a extended AQP2 C terminus, while ubiquitination of AQP2-E258K at K228 will result in a forked C terminus.

To analyze the effect of ubiquitination on AQP2-E258K sorting, we analyzed whether AQP2-K228R-E258K or AQP2-4K>R in MDCK cells colocalized with Lamp2. CLSM analysis revealed that both AQP2-K228R-E258K (Fig. 5c) and AQP2-4K>R (not shown) show an extensive overlap with Lamp2 expression, independent of forskolin stimulation and similar to AQP2-E258K (Fig. 2b). These data reveal that missorting of AQP2-E258K to MVB/Lys occurs independently of its ubiquitination.

## Missorting of AQP2-E258K occurs independently of its increased phosphorylation

S256 in AQP2-E258K is part of a PKA and a PKC phosphorylation consensus site (Fig. 5d). Therefore, either one or both the PKA and PKC pathways may be involved in the increase in S256 phosphorylation in AQP2-E258K. To analyze the role of AQP2-E258K phosphorylation in its missorting, constructs were made in which AQP2-E258K

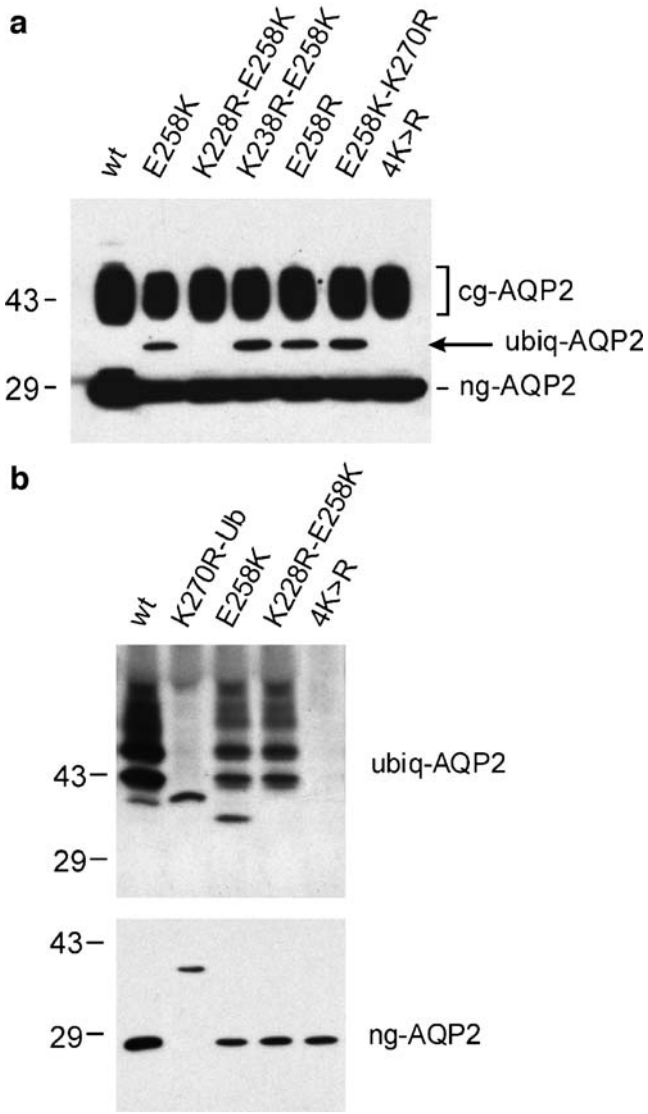


**Fig. 5** Role of S256 phosphorylation and mono-ubiquitination in AQP2-E258K missorting. **a** Lysates of COS-7 cells expressing wt-AQP2 (*wt*), AQP2-E258K (*E258K*), or its indicated mutants were subjected to AQP2 immunoprecipitation, followed by AQP2 immunoblotting. Ubiquitinated (*ubiq-AQP2*), nonglycosylated (*ng-AQP2*), and complex-glycosylated (*cg-AQP2*) pools of AQP2 are indicated. **b** Lysates of MDCK cells stably expressing wt-AQP2 (*wt*), a translation fusion of AQP2-K270R with ubiquitin (*K270R-Ub*), or the indicated AQP2 mutants were subjected to AQP2 immunoprecipitation, followed by ubiquitin (*top panel*) or AQP2 (*lower* panel) immunoblotting. Ubiquitinated (*ubiq-AQP2*) and nonglycosylated (*ng-AQP2*) pools of AQP2 are indicated. The mass of marker proteins in kDa is given on the *left*. **c** MDCK cells stably expressing AQP2-K228R-E258K were grown, fixed, and immuno-labeled as described in Fig. 1. Shown are the single (*AQP2*, *Lamp2*) and merged (*Merge*) confocal images. **d** A one-letter code amino acid alignment of the distal part of the C terminus of AQP2-E258K (*E258K*) and its phosphorylation-state-specific mutants. The introduction of S256D in AQP2-E258K (*E258K-PKA$^{p}$/PKC$^{p}$*) mimics constitutive S256 phosphorylation. The PKA and PKC consensus sites (*PKA-cons., PKC-cons.*), codon 258, the phosphoserine (*Pho* and *rectangle*), and the stopcodon (*asterisk*) are indicated. **e** MDCK cells stably expressing phosphorylation-state specific mutants of AQP2-E258K (indicated on the *left*) were grown and treated as described in the legend of Fig. 1. Shown are the single (*AQP2*, *Lamp2*) and merged (*Merge*) confocal images

can no longer be phosphorylated by PKA (E258K-PKA$^{-}$), PKC (E258Q), or both (E258K-PKA$^{-}$/PKC$^{-}$; Fig. 5d). Furthermore, because in wt-AQP2, S256 phosphorylation is needed for plasma membrane expression [45], a construct was made mimicking AQP2-E258K constitutively phosphorylated at S256 (E258K-PKA$^{p}$/PKC$^{p}$). Finally, because theoretically phosphorylation and ubiquitination may independently cause AQP2-E258K missorting, the K228 was replaced by an arginine in all these mutants. Stable MDCK transfectants were made and subjected to immunofluorescence studies. Confocal analysis revealed that all these mutants colocalized extensively with Lamp2 (Fig. 5e), independent of forskolin stimulation (not shown), indicating that ubiquitination and phosphorylation of AQP2-E258K alone or in combination do not cause the missorting of AQP2-E258K to MVB/Lys.

### Missorting of AQP2-E258K is caused by the loss of the glutamic acid at position 258

Because the observed post-translational modification that occurs specifically with AQP2-E258K seems to be a result of the missorting rather than its cause, the loss of E258 may be the cause of AQP2-E258K missorting. The sorting intolerant from tolerant (SIFT) analysis ([32]; http://blocks.fhcrc.org/sift/SIFT.html) indeed predicts that any substitution for the lysine at position 258 is not tolerated for AQP2 protein function. Besides, the glutamic acid is well conserved between animal species in AQP0, 1, 2, 4 and 5. To study this further, constructs encoding AQP2-E258Q and AQP2-E258A were made and stably expressed in MDCK cells. CLSM analysis indeed revealed that AQP2-E258Q (Fig. 5d,e) and AQP2-E258A (not shown) also colocalize with Lamp2 in MVB/Lys. Altogether, these data clearly indicate that AQP2-E258K missorting is solely caused by the loss of E258.

## Discussion

### Missorting of wt-AQP2/AQP2-E258K complexes to multivesicular bodies/lysosomes explains dominant NDI

In transfected hepatocytes, colocalization studies with organelle marker proteins revealed that AQP2-E258K was expressed in the Golgi apparatus and MVB/Lys [14]. In renal CD8 cells treated with or without forskolin, colocalization with AC17 also suggested lysosomal sorting of

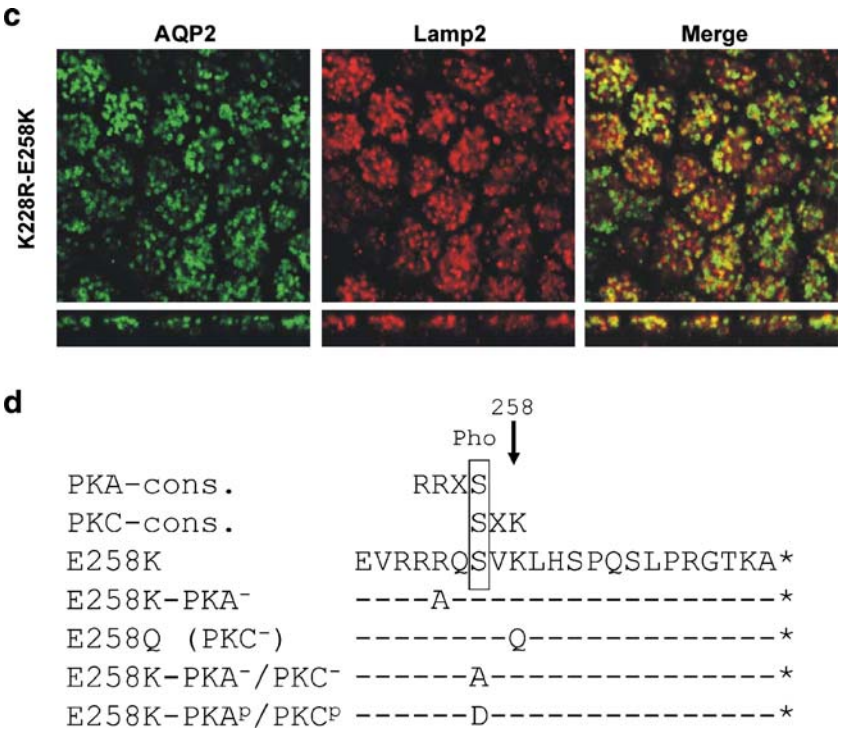


**Fig. 5** (continued)

AQP2-E258K, but because of the inability to detect the trans-Golgi network, localization of AQP2-E258K to this organelle could not be excluded [33]. In our studies, immunocytochemical and cell surface biotinylation experiments of polarized MDCK-AQP2-E258K cells revealed that with or without forskolin stimulation, AQP2-E258K was retained in intracellular compartments and colocalized mainly with the MVB/Lys marker protein, Lamp2 (Figs. 1 and 2). The overlap of AQP2-E258K localization with LysoTracker (Fig. 2d), which accumulates in acidic compartments, as well as the reduced stability of AQP2-E258K compared to wt-AQP2 (Fig. 3), further underscore a MVB/lys localization of AQP2-E258K. In the polarized MDCK cells, however, AQP2-E258K did not colocalize with marker proteins for the *cis*- (Fig. 2), medial-, or *trans*-Golgi network (not shown). In contrast, in nonpolarized MDCK cells, we do observe a localization of wt-AQP2 and AQP2-E258K in the Golgi network [46]. As AQP2-E258K also localizes to the Golgi complex region in oocytes [29], this subcellular localization may be due to the nonpolarized nature of the analyzed cells.

Despite the different localization, AQP2-E258K confers a dominant-negative effect onto the water permeability of wt-AQP2 in oocytes by forming heteroligomers with wt-AQP2 [21, 29], suggesting that this dominant effect is caused by the intracellular retention of wt-AQP2/AQP2-E258K oligomers. Indeed, upon coexpression in MDCK cells, we found that AQP2-E258K interacts with and keeps GFP-tagged wt-AQP2 from the apical membrane (Fig. 2c). Moreover, both AQP2-E258K and GFP-tagged wt-AQP2 were shown to colocalize in LysoTracker-positive compartments (Fig. 2d), indicating that also the wt-AQP2/AQP2-E258K complexes mainly sort to MVB/Lys. Together, these data reveal that AQP2-E258K and wt-AQP2 also interact in MDCK cells, resulting in the sorting of the heteromeric complex to MVB/Lys, thereby providing a cell-biological explanation for the dominant phenotype of NDI in this particular family.

## AQP2-E258K shows a unique form of mono-ubiquitination, which, however, has no role in the MVB/Lys sorting of this mutant

During the past years, the role of mono-ubiquitination in internalization and degradation of membrane proteins in MVB has been increasingly recognized. For example, phosphorylation and monoubiquitination has been implicated in the internalization and degradation of mammalian receptor tyrosine kinases and G-protein-coupled receptors [12, 15, 17, 24, 38], while internalization of the renal epithelial sodium channel ENaC, renal outer medullary potassium channel ROMK, and chloride channel CLC5 involves their ubiquitination [40]. Moreover, we recently found that K63-linked short-chain ubiquitination of wt-AQP2 at K270 mediates both its endocytosis and lysosomal degradation [20]. As ubiquitination occurs on lysines, we therefore anticipated that the MVB/Lys localization of AQP2-E258K could be due to an increased ubiquitination at K258, K270, or another

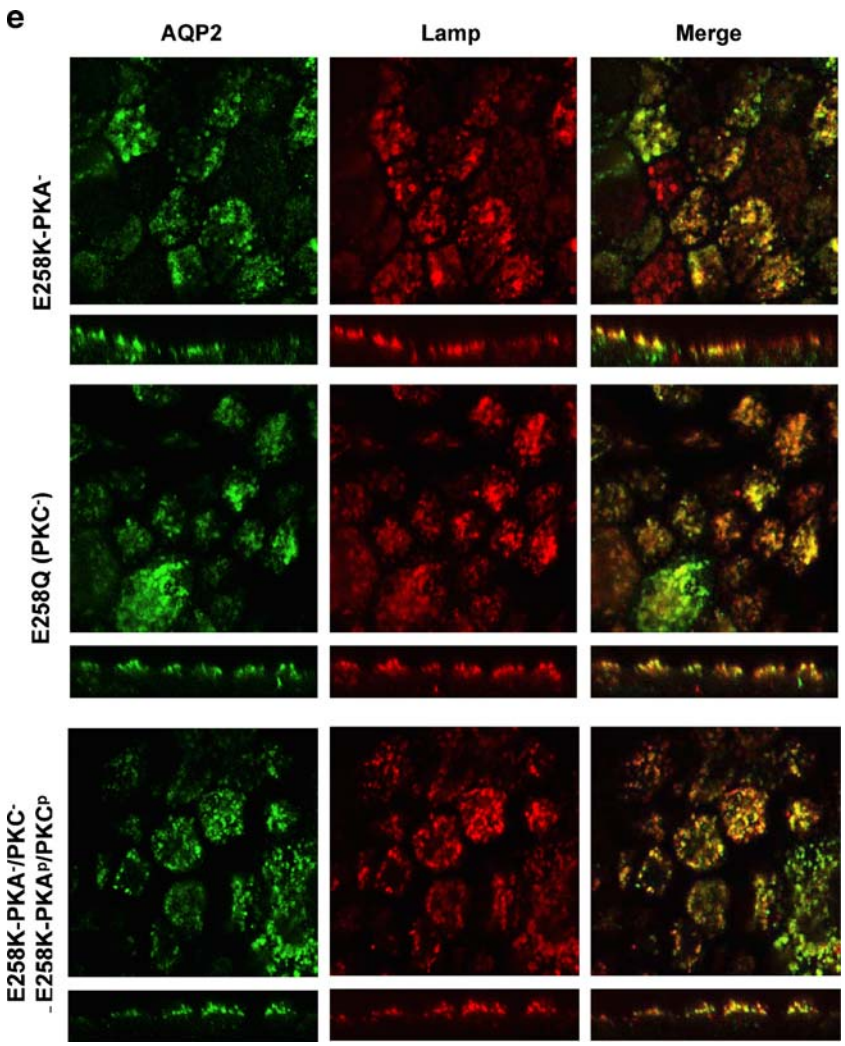


**Fig. 5** (continued)

site. Indeed, in contrast to wt-AQP2, AQP2-E258K appeared to be specifically monoubiquitinated at a novel site, being K228, resulting in a mass increase of AQP2-E258K of ~6 kDa, which is about the mass of one ubiquitin moiety (Figs. 3a, 4a,b, 5a,b; [10]). Furthermore, the presence of this band at 1–6 h after pulse-chase labeling at which time points complex-glycosylated AQP2-E258K (40–45 kDa) was also most prominently present (Fig. 3) indicates that ubiquitination occurs at a post-Golgi complex step in the biosynthesis of AQP2-E258K.

Elimination of this ubiquitination site in AQP2-K228R-E258K, however, did not revoke missorting to MVB/Lys (Fig. 5c). Because AQP2-K228R-E258K is, like wt-AQP2 and AQP2-E258K, still ubiquitinated at K270 (Fig. 5b), one could, however, still speculate that a possible spatial and/or temporal effect of K270R ubiquitination of AQP2-E258K may cause its missorting. This, however, seems unlikely because the mutant in which all cytosolic lysines were replaced by an arginine (AQP2-4K>R) is still missorted to MVB/Lys, despite its undetectable levels of ubiquitination (Fig. 5b,c). Instead, our data suggest that K228 ubiquitination of AQP2-E258K is a result of the MVB/Lys sorting of AQP2-E258K or of just a conformational change of AQP2 introduced by the E258K mutation and contains a warning that ubiquitination of membrane proteins is not always an indication of their role in MVB sorting.

## MVB/lysosomal missorting of AQP2-E258K occurs independent from its phosphorylation at S256

A spatial and temporal phosphorylation may affect the sorting/function of proteins [28, 36]. As the PKA-phosphorylation site S256 is in close proximity to the mutated amino acid E258, we hypothesized that the introduced K258 could interfere with S256 phosphorylation by PKA. Alternatively, a changed spatial or temporal S256 phosphorylation in AQP2-E258K by PKC could be fundamental to the role of AQP2-E258K in dominant NDI

because the E258K substitution introduced a putative phosphorylation site for PKC.

However, the E258K mutation did not interfere with S256 phosphorylation by PKA because forskolin stimulation of orthophosphate-labeled MDCK cells revealed a clear increase in phosphorylated AQP2-E258K, as well as of control wt-AQP2 (Fig. 4). The lack of AQP2-S256A phosphorylation with forskolin furthermore suggested that forskolin phosphorylated S256 only in AQP2-E258K. Our findings are in contrast to those of Procino et al. [33], who detected a small but insignificant increase in phosphorylation of AQP2-E258K upon forskolin treatment. This difference might be due to a high basal cAMP level in their experiments because orthophosphate labeling with forskolin only visualizes the increase in phosphorylation of proteins, and we standardly reduce the basal level of cAMP and AQP2 phosphorylation by adding indomethacin [5].

Moreover and in contrast to wt-AQP2 [45], AQP2-E258K was indeed increased in its phosphorylation by the PKC activator, PMA (Fig. 4a), which suggested that this phosphorylation by PKC might underlie its missorting. The even stronger increase in phosphorylation of AQP2-E258K after simultaneous forskolin and PMA stimulation even suggests to a synergistic phosphorylation of AQP2-E258K by PKA and PKC. Therefore, we designed mutants lacking the PKA consensus site, PKC consensus site, or the S256 phosphorylation site itself. To rule out the possibility that two factors (here, ubiquitination and phosphorylation) independently cause missorting, a phenomenon we have observed for the basolateral sorting of the AQP2-insA mutant in dominant NDI [17], all phosphorylation mutants were made in the AQP2-E258K-ubiquitination-deficient K228R mutant. Nevertheless, all mutants were still mainly sorted to MVB/Lys, indicating that a spatial or temporal phosphorylation of AQP2-E258K at S256 by PKA or PKC is not involved in its missorting to MVB/Lys (Fig. 5e). This was further underscored by the finding that the S256D mutation, which mimics constitutive phosphorylation in wt-AQP2 that results in an apical membrane localization without forskolin stimulation [45], was not able to restore plasma membrane sorting of AQP2-E258K (Fig. 5e).

## Loss of the conserved E258 provides an explanation for AQP2-E258K missorting

While the increased ubiquitination or putatively changed phosphorylation at S256 could not explain MVB/Lys missorting of AQP2-E258K, it is of relevance that AQP2-E258Q (Fig. 5d,e) and AQP2-E258A (not shown) were also sorted to MVB/Lys. Moreover, an amino acid alignment of the C tails of several AQPs revealed that the glutamic acid is highly conserved between mouse, rat, and human AQP0, AQP1, AQP2, AQP4, and AQP5, and SIFT analyses predict that any replacement of E258 in AQP2 or of the aligned glutamic acids in AQP1, AQP4, and AQP5 are deleterious for the involved AQP proteins. These data reveal that it is the lack of E258 rather than the introduction of the lysine (K) that causes AQP2-E258K missorting and indicates for the first time that E258 in AQP2 and possibly its counterparts in AQP0, AQP1, AQP4, and AQP5 is an important amino acid for AQP functioning. The exact role of E258 in AQP2 remains to be established.

In conclusion, we have established that AQP2-E258K alone but also when complexed to wt-AQP2 mainly sorts to MVB/Lys, which provides a cell-biological explanation for the role of AQP2-E258K in dominant NDI. We furthermore found that although AQP2-E258K is additionally mono-ubiquitinated and phosphorylated by PMA-sensitive kinases and that these modifications were not fundamental to its missorting. Instead, just the loss of E258 appeared to be the molecular cause of AQP2-E258K sorting to MVB/Lys.

The structure of the water-pore region and surrounding transmembrane domains of several AQPs has been resolved to atomic resolution [11, 30, 37, 44]. However, while the C-terminal tails of several AQPs play a critical role in their physiology because they determine their translocation to and from the cell surface, their structure and changes therein with physiological stimuli, such as phosphorylation and ubiquitination events, are completely unknown. Our data indicate that E258 is a critical amino acid within the AQP2 tail, and future structural studies have to reveal whether the changed AQP2 structure induced by the loss of E258 resembles to some extent the structure of K270-ubiquitinated AQP2, as both are sorted to MVB/Lys. Moreover, as sorting is often accomplished by interacting proteins, further studies will focus on the identification of wt-AQP2-interacting proteins and proteins that target AQP2-E258K to the MVB/lysosomal compartment.

**Acknowledgments** This research was supported by grants from the Dutch Organization of Scientific Research (NWO-MW 902-18-292) to PMTD and PvdS and to EJK (NWO; 916.36.122) and from the European Union (QLRT-2000-00778, QLK3-CT-2001-00987) to PMTD.

## References

1. Asai T, Kuwahara M, Kurihara H, Sakai T, Terada Y, Marumo F, Sasaki S (2003) Pathogenesis of nephrogenic diabetes. insipidus by aquaporin-2 C-terminus mutations. Kidney Int 64:2–10
2. De Mattia F, Savelkoul PJ, Bichet DG, Kamsteeg EJ, Konings IB, Marr N, Arthus MF, Lonergan M, van Os CH, van der SP, Robertson G, Deen PM (2004) A novel mechanism in recessive nephrogenic diabetes insipidus: wild-type aquaporin-2 rescues the apical membrane expression of intracellularly retained AQP2-P262L. Hum Mol Genet 13:3045–3056

3. De Mattia F, Savelkoul PJ, Kamsteeg EJ, Konings IB, van der SP, Mallmann R, Oksche A, Deen PM (2005) Lack of arginine vasopressin-induced phosphorylation of Aquaporin-2 mutant AQP2-R254L explains dominant nephrogenic diabetes insipidus. J Am Soc Nephrol 16:2872–2880
4. Deen PMT, Croes H, van Aubel RA, Ginsel LA, van Os CH (1995) Water channels encoded by mutant aquaporin-2 genes in nephrogenic diabetes insipidus are impaired in their cellular routing. J Clin Invest 95:2291–2296
5. Deen PMT, Rijss JPL, Mulders SM, Errington RJ, van Baal J, van Os CH (1997) Aquaporin-2 transfection of Madin–Darby canine kidney cells reconstitutes vasopressin-regulated transcellular osmotic water transport. J Am Soc Nephrol 8:1493–1501
6. Deen PMT, Van Balkom BWM, Savelkoul PJ, Kamsteeg EJ, Van Raak M, Jennings ML, Muth TR, Rajendran V, Caplan MJ (2002) Aquaporin-2: COOH terminus is necessary but not sufficient for routing to the apical membrane. Am J Physiol Renal Physiol 282: F330–F340
7. Deen PMT, Verdijk MAJ, Knoers NVAM, Wieringa B, Monnens LAH, van Os CH, van Oost BA (1994) Requirement of human renal water channel aquaporin-2 for vasopressin-dependent concentration of urine. Science 264:92–95
8. Ecelbarger CA, Terris J, Frindt G, Echevarria M, Marples D, Nielsen S, Knepper MA (1995) Aquaporin-3 water channel localization and regulation in rat kidney. Am J Physiol 38: F663–F672
9. Fushimi K, Sasaki S, Marumo F (1997) Phosphorylation of serine 256 is required for cAMP- dependent regulatory exocytosis of the aquaporin-2 water channel. J Biol Chem 272:14800–14804
10. Glickman MH, Ciechanover A (2002) The ubiquitin-proteasome proteolytic pathway: destruction for the sake of construction. Physiol Rev 82:373–428
11. Gonen T, Sliz P, Kistler J, Cheng Y, Walz T (2004) Aquaporin-0 membrane junctions reveal the structure of a closed water pore. Nature 429:193–197
12. Haglund K, Sigismund S, Polo S, Szymkiewicz I, Di Fiore PP, Dikic I (2003) Multiple monoubiquitination of RTKs is sufficient for their endocytosis and degradation. Nat Cell Biol 5:461–466
13. Hendriks G, Koudijs M, van Balkom BW, Oorschot V, Klumperman J, Deen PMT, van der SP (2004) Glycosylation is important for cell surface expression of the water channel aquaporin-2 but is not essential for tetramerization in the endoplasmic reticulum. J Biol Chem 279:2975–2983
14. Hirano K, Zuber C, Roth J, Ziak M (2003) The proteasome is involved in the degradation of different aquaporin-2 mutants causing nephrogenic diabetes insipidus. Am J Pathol 163:111–120
15. Huang F, Kirkpatrick D, Jiang X, Gygi S, Sorkin A (2006) Differential regulation of EGF receptor internalization and degradation by multiubiquitination within the kinase domain. Mol Cell 21:737–748
16. Ikonen E, Tagaya M, Ullrich O, Montecucco C, Simons K (1995) Different requirements for NSF, SNAP, and Rab proteins in apical and basolateral transport in MDCK cells. Cell 81:571–580
17. Kamsteeg EJ, Bichet DG, Konings IB, Nivet H, Lonergan M, Arthus MF, van Os CH, Deen PMT (2003) Reversed polarized delivery of an aquaporin-2 mutant causes dominant nephrogenic diabetes insipidus. J Cell Biol 163:1099–1109
18. Kamsteeg EJ, Deen PMT (2000) Importance of aquaporin-2 expression levels in genotype -phenotype studies in nephrogenic diabetes insipidus. Am J Physiol Renal Physiol 279:F778–F784
19. Kamsteeg EJ, Heijnen I, van Os CH, Deen PMT (2000) The subcellular localization of an Aquaporin-2 tetramer depends on the stoichiometry of phosphorylated and nonphosphorylated monomers. J Cell Biol 151:919–930
20. Kamsteeg EJ, Hendriks G, Boone M, Konings IB, Oorschot V, van der SP, Klumperman J, Deen PM (2006) Short-chain ubiquitination mediates the regulated endocytosis of the aquaporin-2 water channel. Proc Natl Acad Sci USA 103: 18344–18349
21. Kamsteeg EJ, Wormhoudt TA, Rijss JPL, van Os CH, Deen PMT (1999) An impaired routing of wild-type aquaporin-2 after tetramerization with an aquaporin-2 mutant explains dominant nephrogenic diabetes insipidus. EMBO J 18:2394–2400
22. Katsura T, Gustafson CE, Ausiello DA, Brown D (1997) Protein kinase A phosphorylation is involved in regulated exocytosis of aquaporin-2 in transfected LLC-PK1 cells. Am J Physiol 41:F816–F822
23. Kuwahara M, Iwai K, Ooeda T, Igarashi T, Ogawa E, Katsushima Y, Shinbo I, Uchida S, Terada Y, Arthus MF, Lonergan M, Fujiwara TM, Bichet DG, Marumo F, Sasaki S (2001) Three families with autosomal dominant nephrogenic diabetes insipidus caused by aquaporin-2 mutations in the C-terminus. Am J Hum Genet 69:738–748
24. Marchese A, Benovic JL (2001) Agonist-promoted ubiquitination of the G protein-coupled receptor CXCR4 mediates lysosomal sorting. J Biol Chem 276:45509–45512
25. Marr N, Bichet DG, Hoefs S, Savelkoul PJ, Konings IB, De Mattia F, Graat MP, Arthus MF, Lonergan M, Fujiwara TM, Knoers NVAM, Landau D, Balfe WJ, Oksche A, Rosenthal W, Muller D, van Os CH, Deen PMT (2002) Cell-biologic and functional analyses of five new aquaporin-2 missense mutations that cause recessive nephrogenic diabetes insipidus. J Am Soc Nephrol 13:2267–2277
26. Marr N, Bichet DG, Lonergan M, Arthus MF, Jeck N, Seyberth HW, Rosenthal W, van Os CH, Oksche A, Deen PMT (2002) Heteroligomerization of an Aquaporin-2 mutant with wild-type Aquaporin- 2 and their misrouting to late endosomes/lysosomes explains dominant nephrogenic diabetes insipidus. Hum Mol Genet 11:779–789
27. McDill BW, Li SZ, Kovach PA, Ding L, Chen F (2006) Congenital progressive hydronephrosis (cph) is caused by an S256L mutation in aquaporin-2 that affects its phosphorylation and apical membrane accumulation. Proc Natl Acad Sci USA 103:6952–6957
28. Molloy SS, Thomas L, Kamibayashi C, Mumby MC, Thomas G (1998) Regulation of endosome sorting by a specific PP2A isoform. J Cell Biol 142:1399–1411
29. Mulders SM, Bichet DG, Rijss JPL, Kamsteeg EJ, Arthus MF, Lonergan M, Fujiwara M, Morgan K, Leijendekker R, van der Sluijs P, van Os CH, Deen PMT (1998) An aquaporin-2 water channel mutant which causes autosomal dominant nephrogenic diabetes insipidus is retained in the Golgi complex. J Clin Invest 102:57–66
30. Murata K, Mitsuoka K, Hirai T, Walz T, Agre P, Heymann JB, Engel A, Fujiyoshi Y (2000) Structural determinants of water permeation through aquaporin-1. Nature 407:599–605
31. Nabi IR, Le Bivic A, Fambrough D, Rodriguez-Boulan E (1991) An endogenous MDCK lysosomal membrane glycoprotein is targeted basolaterally before delivery to lysosomes. J Cell Biol 115:1573–1584
32. Ng PC, Henikoff S (2003) SIFT: Predicting amino acid changes that affect protein function. Nucleic Acids Res 31:3812–3814
33. Procino G, Carmosino M, Marin O, Brunati AM, Contri A, Pinna LA, Mannucci R, Nielsen S, Kwon TH, Svelto M, Valenti G (2003) Ser-256 phosphorylation dynamics of Aquaporin 2 during maturation from the ER to the vesicular compartment in renal cells. FASEB J 17:1886–1888
34. Robertson GL (1995) Diabetes insipidus. Endocrinol Metab Clin North Am 24:549–572
35. Rosenthal W, Seibold A, Antaramian A, Lonergan M, Arthus M-F, Hendy GN, Birnbaumer M, Bichet DG (1992) Molecular identification of the gene responsible for congenital nephrogenic diabetes insipidus. Nature 359:233–235
36. Sabatini DD, Adesnik M, Ivanov IE, Simon JP (1996) Mechanism of formation of post Golgi vesicles from TGN membranes:

Arf-dependent coat assembly and PKC-regulated vesicle scission. Biocell 20:287–300
37. Schenk AD, Werten PJ, Scheuring S, de Groot BL, Muller SA, Stahlberg H, Philippsen A, Engel A (2005) The 4.5A Structure of Human AQP2. J Mol Biol 350:278–289
38. Shenoy SK, McDonald PH, Kohout TA, Lefkowitz RJ (2001) Regulation of receptor fate by ubiquitination of activated beta 2-adrenergic receptor and beta-arrestin. Science 294:1307–1313
39. Sohara E, Rai T, Yang SS, Uchida K, Nitta K, Horita S, Ohno M, Harada A, Sasaki S, Uchida S (2006) Pathogenesis and treatment of autosomal-dominant nephrogenic diabetes insipidus caused by an aquaporin 2 mutation. Proc Natl Acad Sci USA 103: 14217–14222
40. Staub O, Rotin D (2006) Role of ubiquitylation in cellular membrane transport. Physiol Rev 86:669–707
41. Subramaniam VN, Krijnse-Locker J, Tang BL, Ericsson M, Yusoff AR, Griffiths G, Hong W (1995) Monoclonal antibody HFD9 identifies a novel 28 kDa integral membrane protein on the cis-Golgi. J Cell Sci 108:2405–2414
42. Terris J, Ecelbarger CA, Marples D, Knepper MA, Nielsen S (1995) Distribution of aquaporin-4 water channel expression within rat kidney. Am J Physiol 38:F775–F785
43. Thomsen P, van Deurs B, Norrild B, Kayser L (2000) The HPV16 E5 oncogene inhibits endocytic trafficking. Oncogene 19:6023–6032
44. Tornroth-Horsefield S, Wang Y, Hedfalk K, Johanson U, Karlsson M, Tajkhorshid E, Neutze R, Kjellbom P (2006) Structural mechanism of plant aquaporin gating. Nature 439:688–694
45. Van Balkom BWM, Savelkoul PJ, markovich D, Hofman E, Nielsen S, van der Sluijs P, Deen PMT (2002) The role of putative phosphorylation sites in the targeting and shuttling of the aquaporin-2 water channel. J Biol Chem 277:41473–41479
46. van Beest M, Robben JH, Savelkoul PJ, Hendriks G, Devonald MA, Konings IB, Lagendijk AK, Karet F, Deen PM (2006) Polarisation, key to good localisation. Biochim Biophys Acta 1758:1126–1133
47. van den Ouweland AM, Dreesen JC, Verdijk MAJ, Knoers NVAM (1992) Mutations in the vasopressin type 2 receptor gene (AVPR2) associated with Nephrogenic Diabetes Insipidus. Nat Genet 2:99–102
48. van Lieburg AF, Verdijk MAJ, Knoers NVAM, van Essen AJ, Proesmans W, Mallmann R, Monnens LAH, van Oost BA, van Os CH, Deen PMT (1994) Patients with autosomal nephrogenic diabetes insipidus homozygous for mutations in the aquaporin 2 water-channel gene. Am J Hum Genet 55:648–652